

Photoresponse of PbS nanoparticles–quaterthiophene films prepared by gaseous deposition as probed by XPS

Michael W. Majeski, F. Douglas Pleticha, Igor L. Bolotin, Luke Hanley, Eda Yilmaz et al.

Citation: *J. Vac. Sci. Technol. A* **30**, 04D109 (2012); doi: 10.1116/1.4709386

View online: <http://dx.doi.org/10.1116/1.4709386>

View Table of Contents: <http://avspublications.org/resource/1/JVTAD6/v30/i4>

Published by the AVS: Science & Technology of Materials, Interfaces, and Processing

Related Articles

Comparison of surface photovoltage behavior for n-type versus p-type GaN

J. Vac. Sci. Technol. B **29**, 041205 (2011)

Transport and structural properties of silicon films in the amorphous-to-microcrystalline transition region

J. Vac. Sci. Technol. A **27**, 436 (2009)

Thin-film photovoltaics

J. Vac. Sci. Technol. A **23**, 1208 (2005)

Terahertz magneto-photoconductive characterization of hydrogenic barrier donors in GaAs/AlGaAs epitaxial thin films

J. Vac. Sci. Technol. B **22**, 1580 (2004)

Measurement of charge-separation potentials in GaAs_{1-x}N_x

J. Vac. Sci. Technol. A **21**, 1765 (2003)

Additional information on *J. Vac. Sci. Technol. A*

Journal Homepage: <http://avspublications.org/jvsta>

Journal Information: http://avspublications.org/jvsta/about/about_the_journal


Top downloads: http://avspublications.org/jvsta/top_20_most_downloaded

Information for Authors: http://avspublications.org/jvsta/authors/information_for_contributors

ADVERTISEMENT


Instruments for advanced science

Gas Analysis



- dynamic measurement of reaction gas streams
- catalysis and thermal analysis
- molecular beam studies
- dissolved species probes
- fermentation, environmental and ecological studies

Surface Science




- UHV TPD
- SIMS
- end point detection in ion beam etch
- elemental imaging - surface mapping

Plasma Diagnostics



- plasma source characterization
- etch and deposition process reaction kinetic studies
- analysis of neutral and radical species

Vacuum Analysis



- partial pressure measurement and control of process gases
- reactive sputter process control
- vacuum diagnostics
- vacuum coating process monitoring

contact Hiden Analytical for further details

HIDEN ANALYTICAL

info@hideninc.com
www.HidenAnalytical.com
CLICK to view our product catalogue

Photoresponse of PbS nanoparticles–quaterthiophene films prepared by gaseous deposition as probed by XPS

Michael W. Majeski, F. Douglas Pleticha, Igor L. Bolotin, and Luke Hanley^{a)}

Department of Chemistry, University of Illinois at Chicago, 4500 SES, 845 W. Taylor St., Chicago, Illinois 60607-7061

Eda Yilmaz and Sefik Suzer

Department of Chemistry, Bilkent University, 06800 Ankara, Turkey

(Received 11 January 2012; accepted 14 April 2012; published 1 May 2012)

Semiconducting lead sulfide (PbS) nanoparticles were cluster beam deposited into evaporated quaterthiophene (4T) organic films, which in some cases were additionally modified by simultaneous 50 eV acetylene ion bombardment. Surface chemistry of these nanocomposite films was first examined using standard x-ray photoelectron spectroscopy (XPS). XPS was also used to probe photoinduced shifts in peak binding energies upon illumination with a continuous wave green laser and the magnitudes of these peak shifts were interpreted as changes in relative photoconductivity. The four types of films examined all displayed photoconductivity: 4T only, 4T with acetylene ions, 4T with PbS nanoparticles, and 4T with both PbS nanoparticles and acetylene ions. Furthermore, the ion-modified films displayed higher photoconductivity, which was consistent with enhanced bonding within the 4T organic matrix and between 4T and PbS nanoparticles. PbS nanoparticles displayed higher photoconductivity than the 4T component, regardless of ion modification. © 2012 American Vacuum Society. [<http://dx.doi.org/10.1116/1.4709386>]

I. INTRODUCTION

The goal of efficient, low cost solar energy conversion has motivated many investigations of nanostructured materials for photovoltaic applications.^{1–3} Organic–inorganic hybrids are one promising class of novel materials that combine organic components and inorganic nanostructures through chemical and/or physical interactions.⁴ Organic films containing lead chalcogenide nanoparticles are one such hybrid material that have been the subject of intense study.^{2,5,6} Lead sulfide (PbS) nanoparticles allow for a size tunable bandgap due to quantum confinement effects, have large extinction coefficients,⁷ and are thus under consideration for use as the near-IR active layer in multijunction photovoltaics.⁵

This paper discusses the analysis of nanocomposite films of PbS nanoparticles in quaterthiophene (4T) that were prepared by a combination of cluster beam, physical vapor, and ion-assisted deposition. Cluster beam deposition (CBD) allows direct control of nanoparticle properties, including surface chemistry and matrix environment.^{8,9} CBD can also be used to prepare films with predetermined thicknesses and additionally allows indirect control of film morphology. CBD is performed under vacuum, reducing oxidation effects on the deposited films and nanoparticles therein. Control of oxidation is significant as it has been argued that films of surface oxidized PbS nanoparticles behave as photodetectors rather than photovoltaics.⁵

Cluster beam deposition of PbS nanoparticles was performed simultaneously with evaporative deposition of the organic phase, as well as with the addition of 50 eV acetylene ion bombardment (predominantly $C_2H_x^+$), as shown sche-

matically in Fig. 1. Ion modification shares some characteristics with plasma polymerization, which has been previously used for surface modification of nanoparticles.¹⁰ The acetylene ions used in ion-assisted deposition behave both as catalysts and reagents by energetically inducing bonding between condensed phase species and forming adducts with the neutral reagents.^{11–15}

X-ray photoelectron spectroscopy (XPS) was employed to probe photoconductivity of the PbS nanoparticle–4T composite films. For insulating and semiconducting samples, it has been observed that surface charging can shift the measured binding energies in an X-ray photoelectron (XP) spectrum.^{16–19} Ineffective filling of holes due to photoemission results in the buildup of a positive surface potential. Monitoring the shifts in XP spectra due to this surface charge buildup allows for examination of changes in the local electrical conductance of different components in a sample.

The use of XPS for probing photovoltaic effects in heterostructured materials has been reported in various works.^{20–24} Surface potential shifts related to external electron gun stimulation and/or illumination via laser or other light sources are observable in XP spectra of composite semiconductor surfaces.²⁵ For such surfaces, it has been demonstrated that photovoltaic and photoconductive properties are related to static or quasistatic shifts of XPS peaks. Furthermore, these shifts can be qualitatively studied by using films on conductive substrates. This XPS technique examines the charging/discharging process during laser illumination, without the need for metal overlayers to complete electrical contact with these delicate nanocomposite films. It is hypothesized that the surface chemistry and heterojunction bonding within the nanocomposite films affect photocharging, and in turn can be probed by XPS. XPS measurements performed upon green laser

^{a)}Electronic mail: lhlanley@uic.edu

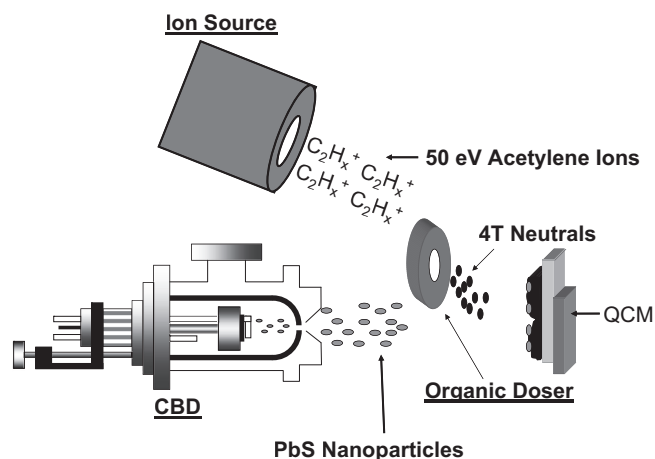


Fig. 1. Schematic of cluster beam deposition (CBD) of PbS nanoparticles combined with evaporation of 4T neutrals and acetylene ion modification.

illumination, as shown schematically in Fig. 2, were employed here to compare PbS nanoparticle–4T composite films prepared with and without acetylene ion modification.

II. EXPERIMENT

A. Sample preparation

Sample preparation was performed in Chicago, IL, using the methods shown schematically in Fig. 1. Silicon wafers [P-doped, *n*-type Si (100) wafers, Atomergic Chemical Corporation, Melville, NY] were used as substrates and were hydrogen terminated by hydrofluoric acid etching to leave at most a minimal oxide layer. PbS clusters were formed in a magnetron condensation source by reactively sputtering a Pb metal target in an Ar/H₂S gas mixture, as previously described.^{8,9} The gaseous PbS clusters were simultaneously deposited onto the Si substrate with oligothiophene (sexithiophene, CAS 88493-55-4, Sigma-Aldrich, St. Louis, MO) evaporated from a heated ceramic crucible (LTE 11 000 K, 1 cc, Kurt J. Lesker, Pittsburgh, PA). The oligothiophene sublimation temperature was varied from 413 to 513 K to maintain a 1:1 fluence with the PbS clusters, as monitored with a quartz crystal microbalance. While the oligothiophene sample purchased was nominally sexithiophene, mass spectrometric analyses (not shown, to be presented elsewhere) found that predominantly quaterthiophene was thermally evaporated onto the substrates. This

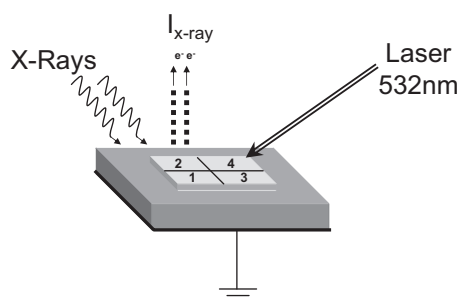


Fig. 2. Schematic representation of XPS measurements performed here. Region 1 is 4T only, region 2 is 4T with acetylene ions (4T + ions), region 3 is 4T with PbS nanoparticles (4T + PbS), and region 4 is 4T with both PbS nanoparticles and acetylene ions (4T + PbS + ion).

resulted from the lower sublimation temperature of 4T compared with sexithiophene and the ~10% 4T content of the oligothiophene mixture as received from the vendor (as verified by mass spectrometric analysis).

Acetylene ions with 50 eV kinetic energy were generated by a Kaufman ion source (IBS 250, 3 cm, Veeco/Commonwealth Scientific, Plainview, NY)¹⁵ and used to modify the films simultaneous with 4T and PbS cluster deposition. The ion source was mounted ~45° from the surface normal. An aperture was placed directly in front of the sample perpendicular to the organic doser and 37° from the normal of the CBD source. The metal aperture allowed for four different distinct regions to be deposited simultaneously onto the Si substrate, as shown in Fig. 2. The four regions were 4T only, 4T with acetylene ions (denoted as 4T + ions), 4T with PbS nanoparticles (denoted as 4T + PbS), and 4T with both PbS nanoparticles and acetylene ions (denoted as 4T + PbS + ion). The films were made in three replicate samples for analysis.

B. XPS analyses

X-ray photoelectron spectra were collected in Ankara, Turkey using a commercial XPS spectrometer (K-Alpha, Thermo Fisher Scientific) with monochromatized Al *K* α x-ray source. The spectrometer was able to probe the sample with a small x-ray spot size between 30 and 400 μ m. All core level spectra were charge referenced to C 1s, taken to be at 285.0 eV, and fit using commercial software (XPS PEAK FIT 4.1). The instrument was also equipped with a flood gun as an external electron source and an additional argon ion source for neutralization of the sample surface. The electron flood gun was operated at 0.5 eV and 100 mA for all the measurements reported in this work. The sample holder was grounded and samples held by Au clamps. The optical stimulus was provided by a continuous wave (cw) 532 nm (2.3 eV) green laser outputting 50 mW (GCL532, CrystalLaser, Reno, NV). The schematic in Fig. 2 represents the photoilluminated XPS measurement.^{24,26}

III. RESULTS AND DISCUSSION

A. Elemental and chemical analysis of films

The survey x-ray photoelectron spectra (not shown) verified the composition of the nanocomposite films as consisting of Pb, S, and C with only a small O signal due to minor oxidation. The average elemental composition for all three samples and four regions is presented in Table I. Although samples were kept under vacuum after preparation, they were sent from Chicago to Ankara and thus were exposed to atmosphere, which caused some oxidation. Carbon content increased slightly for films with ion modification compared to those without, as expected upon the introduction of carbonaceous acetylene ions. Correspondingly, the Pb and S components from all contributions for ion-modified films slightly decreased. Introduction of PbS nanoparticles led to the appearance of a Pb peak. Oxygen content also slightly increased for ion-modified films, likely due to the formation of oxidizable radical sites.

The quoted errors in the elemental compositions of Table I reflect sample-to-sample fluctuations in film thicknesses,

TABLE I. Elemental composition of four different types of quaterthiophene (4T) films: with (4T + ion) and without (4T) ion bombardment as well as with PbS nanoparticles (4T + PbS + ion and 4T + PbS, respectively).

Film region	Percent composition						
	%O	%Pb	%C	%S _{4T}	%S _{4T-PbS}	%S _{PbS-Surf}	%S _{PbS-Core}
4T	3.5 ± 0.9	—	74.3 ± 1.7	22.2 ± 1.4	—	—	—
4T + ion	7.4 ± 1.3	—	76.0 ± 1.8	16.6 ± 1.3	—	—	—
4T + PbS	6.8 ± 1.9	7.3 ± 3.3	67.4 ± 3.9	8.0 ± 2.2	5.2 ± 1.4	1.9 ± 0.6	3.4 ± 1.6
4T + PbS + ion	6.7 ± 1.8	4.7 ± 1.4	73.2 ± 3.7	6.9 ± 2.0	5.0 ± 0.5	1.3 ± 0.3	2.2 ± 0.8

PbS/4T ratios, and/or the oligomer distribution. A slight variation in the Pb to S ratios for the unmodified and ion-modified areas was also observed for different samples. This variation may have arisen from sample heating and/or ion-induced degradation by the ion source, which could have led to evaporation of a small portion of the film simultaneous with deposition.

The S 2*p* core level spectra of PbS nanoparticle–4T films with and without ion bombardment are shown in Fig. 3. The S 2*p* core level spectra were deconvoluted into four major sources of sulfur; in addition to the 2:1 spin orbit splitting for S 2*p*_{3/2}:S 2*p*_{1/2} from each individual component. These four components were assigned as S_{4T} arising from 4T at binding energy of 164.3 eV, S_{4T-PbS} arising from 4T interacting with the PbS nanoparticle at 163.7 eV, S_{PbS-Surf}, which is the surface component of PbS at 162.2 eV, and S_{PbS-Core}, which is the core component of PbS at 161.3 eV.⁸

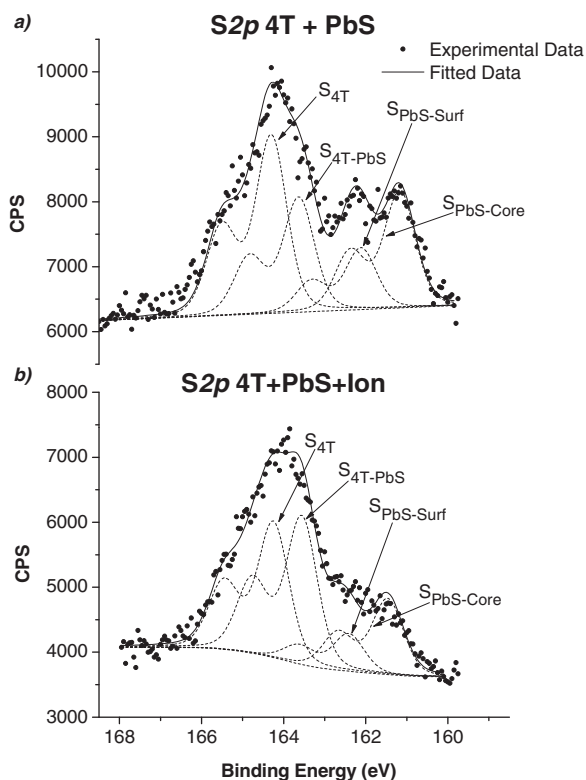


Fig. 3. S 2*p* core level spectra of PbS nanoparticles cluster beam deposited into 4T (a) without and (b) with 50 eV acetylene ($C_2H_x^+$) ion modification. Broken lines are fits to individual components (see the text) and solid lines are composite fit. Closed points are actual data.

Comparison of core level spectra on samples with and without $C_2H_x^+$ ion modification indicates enhanced bonding within the nanocomposite film. The ratio of S_{4T-PbS}/Pb for the 4T + PbS samples was 0.7 ± 0.4 , but this ratio increased to 1.1 ± 0.3 for the 4T + PbS + ion samples, indicating that ion modification increased the coupling between the nanoparticles and 4T. Further experiments on samples that were only minimally air exposed supported the increase in nanoparticle–4T bonding (results not shown, but to be presented elsewhere).

Attempts to extract functional group information from the C 1*s* peak failed, as this component did not shift significantly for the various changes in chemical environment occurring here.¹³ Thus, the C 1*s* peak was fit with a single component.

Film and nanoparticle morphology was not directly examined here. Prior work showed that well-separated, 3.5 ± 0.9 nm diameter PbS nanoparticles with some degree of crystallinity were formed under conditions similar to those used to prepare the 4T + PbS films.⁸ Those experiments were performed by depositing nanoparticles and organic oligomer onto copper grids for subsequent analysis by dark field scanning transmission electron microscopy. However, more recent attempts to examine changes in film morphology by transmission electron microscopy were hindered by the erosion of the copper grids by acetylene ion bombardment. Further studies of film morphology for the 4T + PbS + ion films are under consideration.

B. XPS analysis of core level shifts due to green laser illumination

All four types of films—4T, 4T + ion, 4T + PbS, and 4T + PbS + ion—showed photoinduced shifts in their core levels. Furthermore, smaller shifts were observed for the ion-modified films, consistent with improved charge transfer and increased photoconductivity. These photoinduced XPS results suggest that ion-assisted deposition leads to enhanced bonding within the 4T organic matrix as well as between the organic matrix and PbS nanoparticles.

The shifts of elemental core spectra due to green laser excitation were measured with the averages of the shifts for all three replicate samples in all four regions presented in Table II. Typical S 2*p* and Pb 4*f* spectra in the regions of 4T with PbS nanoparticles with and without ions are shown in Figs. 4 and 5. As seen in Figs. 4 and 5, the dashed lines show the XPS peaks shifting toward higher binding energy for all laser illuminated spectra. Illumination creates a positive potential on the sample surface, which shifts the binding energy of photoelectrons. Increased photoconductivity in the

TABLE II. Average calculated peak shifts (eV) upon green laser excitation for core level spectra.

Peak	Sample region			
	4T + PbS	4T + PbS + ion	4T	4T + ion
S 2p _{4T}	0.43 ± 0.1	0.25 ± 0.1	0.50 ± 0.03	0.35 ± 0.1
S 2p _{4T-PbS}	0.45 ± 0.1	0.23 ± 0.2		
S 2p _{PbS-Core+Surf}	0.33 ± 0.1	0.13 ± 0.2		
C 1s	0.41 ± 0.1	0.25 ± 0.1	0.52 ± 0.03	0.37 ± 0.1
Pb 4f	0.37 ± 0.1	0.19 ± 0.1		

film causes core level peaks to shift back toward their native binding energies for positively charged surfaces, reducing the shift induced by illumination.^{23,26}

Ion modification shows a decrease in core level shifts in 4T films with and without PbS nanoparticles due to laser illumination. For example, the 4T + PbS + ion films revealed a decreased shift in all core level spectra compared to the 4T + PbS (no ion-modification) film, indicating a more photoconductive film is formed by ion modification.

The shift of PbS core and surface components of the S 2p components were fixed to each other during fitting; therefore, both peaks shift the same amount in this interpretation and their shift is given as S 2p_{PbS-Core+Surf} in Table II. Differences in peak shifts for different components were small, but the S 2p_{PbS-Core+Surf} component shifted slightly less than the other components and core levels (at least in the absence of ion

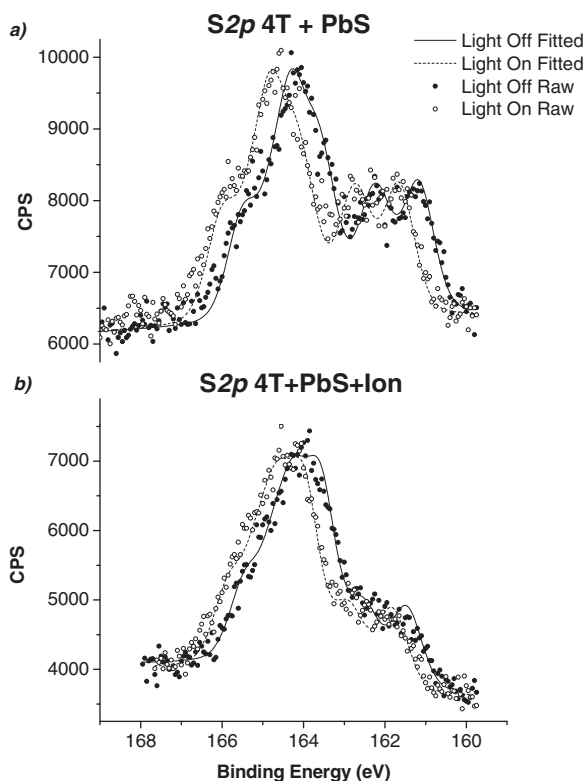


FIG. 4. S 2p core level XP spectra of the PbS nanoparticle with 4T films (4T + PbS) on Si wafer (a) without and (b) with 50 eV acetylene ion-assisted deposition. Solid lines are fits and closed points are data without illumination, while dashed lines are fits and open points are data with green cw laser illumination.

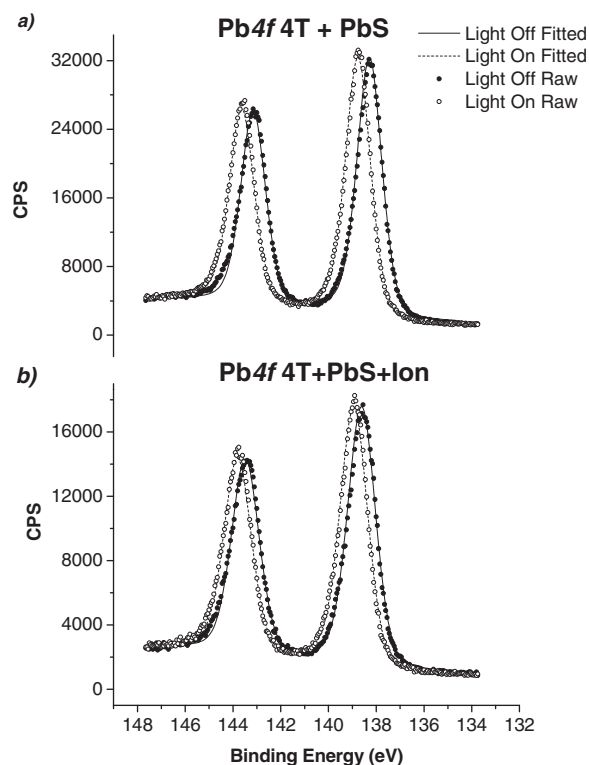


FIG. 5. Pb 4f core level XP spectra of the PbS nanoparticle with 4T films (4T + PbS) on Si wafer (a) without and (b) with 50 eV acetylene ion-assisted deposition. Solid lines are fits and closed points are data without illumination, while dashed lines are fits and open points are data with green cw laser illumination. The Pb 4f peaks were fit with only one component.

modification). This observation of differential charging is consistent with a slightly higher photoconductivity for PbS nanoparticles compared with the 4T film. While the smaller photoinduced shift in the S 2p_{PbS-Core+Surf} is on the order of the reported errors, those quoted errors actually reflect fluctuations in the film thickness and/or composition (see previous discussion). Examination of the photoinduced shifts for each of the samples showed that the S 2p_{PbS-Core+Surf} shift was always ~0.1 eV smaller than the other shifts. Note that the binding energies can be measured to ±0.02 eV.

Photoconductivity is the convolution of the number of carriers generated per absorbed photon and how fast a carrier moves through the medium under applied field.²⁷ If the conductivity of the surface layer is increased by illumination with an external light source, surface charge decreases due to compensation by available charge carriers.²³ Increased photoconductivity is observed here in the reduced binding energy shifts upon laser illumination.

The most likely explanation for the increase in photoconductivity is an increase in chemical bonding, which creates larger conjugated systems that in turn allow increased intramolecular charge transfer. Enhanced bonding in ion-assisted deposition of oligothiophenes has been observed previously^{11–13} and was predicted by molecular dynamic simulations.¹⁴ Ongoing work is exploring a similar mechanism in which the 4T + PbS + ion films display enhanced covalent bonding between the PbS nanoparticles and the 4T phase, induced by ion-assisted modification.

An alternative explanation for the increase in photoconductivity due to the ion-assisted deposition could arise from an increase in available free charge carriers with the addition of $C_2H_x^+$ to the system and an enhancement in charge generation efficiency (i.e., intermolecular charge transfer). However, the validity of this mechanism requires the deposited ions to maintain at least part of their gaseous-state charge upon deposition into the film.

It is known that light-induced carrier generation and diffusion may cause band bending in semiconductors such as doped Si wafers.²³ Photoillumination in semiconductors with a light source whose energy is larger than that of the semiconductors' bandgap can be described as decreasing band-bending via creation of additional electron–hole pairs, resulting in a further increase in binding energy.^{25,28} A similar photoinduced behavior could be expected for the intrinsically semiconducting PbS nanoparticles, given a bandgap of ~ 1.4 eV for the ~ 3 nm PbS nanocrystals²⁹ and 2.3 eV excitation energy of the green laser employed here. However, it is thought that the nanocomposite films studied here exhibit charging shifts mainly due to their significant resistivity. Differentiation between these two processes is not possible with the experiments performed here. It should also be noted that the thickness of these films is ~ 100 nm, and the underlying Si substrate was not seen in any XP spectra. Therefore, any photoinduced charging that might have occurred in the Si wafer could not be observed due to the inability of the Si photoelectrons to escape through the nanocomposite film during the XPS measurement.

IV. SUMMARY AND CONCLUSIONS

These experiments demonstrate that cluster beam deposition of semiconductor nanoparticles combined with physical deposition of an organic oligomer can prepare films with a measurable photoinduced response. Furthermore, it is found that this photoinduced response, a type of photoconductivity, can be increased by ion-assisted deposition. The increase in photoconductivity with ion-assisted deposition is analogous to the changes in photodetector and photovoltaic properties of films containing PbS or PbSe nanoparticles observed following chemical or thermal control of the organic ligands on the nanoparticle surfaces.^{30–32} Also, a differential charging event is observed here in which the semiconductor nanoparticles display enhanced photoconductivity compared with the surrounding organic matrix. The cluster beam deposition and ion-assisted deposition strategies can prepare a wide variety of nanocomposite films, indicating their broad potential for photovoltaic and photoconductive applications.

ACKNOWLEDGMENTS

The equipment used for deposition of PbS was obtained using funds from the U.S. Department of Defense under Contract No. W81XWH-05-2-0093. The University of Illinois at Chicago also provided support for this work as well as funds for M.M. to travel to Ankara to assist in the XPS analyses.

- ¹P. V. Kamat, *J. Phys. Chem. C* **112**, 18737 (2008).
- ²H. W. Hillhouse and M. C. Beard, *Curr. Opin. Colloid Interface Sci.* **14**, 245 (2009).
- ³J. Chandrasekaran, D. Nithyaprakash, K. B. Aijan, S. Maruthamuthu, D. Manoharan, and S. Kumar, *Renewable Sustainable Energy Rev.* **15**, 1228 (2011).
- ⁴R. Faccio, L. Fernandez-Werner, H. Pardo, and A. W. Momburu, *Recent Pat. Nanotechnol.* **5**, 46 (2011).
- ⁵E. H. Sargent, *Adv. Mater.* **20**, 3958 (2008).
- ⁶A. J. Nozik, *Chem. Phys. Lett.* **457**, 3 (2008).
- ⁷L. Cademartiri, E. Montanari, G. Calestani, A. Migliori, A. Guagliardi, and G. A. Ozin, *J. Am. Chem. Soc.* **128**, 10337 (2006).
- ⁸A. M. Zachary, I. L. Bolotin, D. J. Asunskis, A. T. Wroble, and L. Hanley, *ACS Appl. Mater. Interfaces* **1**, 1770 (2009).
- ⁹A. M. Zachary, I. L. Bolotin, and L. Hanley, in *Nanofabrication Using Focused Ion and Electron Beams: Principles and Applications*, edited by S. Moshkalev (Oxford University Press, New York, 2011).
- ¹⁰L. Cademartiri, A. Ghadimi, and G. A. Ozin, *Acc. Chem. Res.* **41**, 1820 (2008).
- ¹¹S. Tepavcevic, Y. Choi, and L. Hanley, *Langmuir* **20**, 8754 (2004).
- ¹²S. Tepavcevic, W.-D. Hsu, S. B. Sinnott, and L. Hanley, *Mater. Res. Soc. Symp. Proc.* **937**, M03 (2006).
- ¹³S. Tepavcevic, A. T. Wroble, M. Bissen, D. J. Wallace, Y. Choi, and L. Hanley, *J. Phys. Chem. B* **109**, 7134 (2005).
- ¹⁴W.-D. Hsu, S. Tepavcevic, L. Hanley, and S. B. Sinnott, *J. Phys. Chem. C* **111**, 4199 (2007).
- ¹⁵A. M. Zachary, Y. Choi, M. Drabik, I. L. Bolotin, H. Biederman, and L. Hanley, *J. Vac. Sci. Technol. A* **26**, 212 (2008).
- ¹⁶A. Cros, *J. Electron Spectrosc. Relat. Phenom.* **59**, 1 (1992).
- ¹⁷I. Doron-Mor, A. Hatzor, A. Vaskevich, T. van der Boom-Moav, A. Shanzer, I. Rubinstein, and H. Cohen, *Nature (London)* **406**, 382 (2000).
- ¹⁸S. Suzer, *Anal. Chem.* **75**, 7026 (2003).
- ¹⁹P. M. A. Sherwood, *Surf. Sci.* **600**, 771 (2006).
- ²⁰R. Buller, H. Cohen, E. Minkin, R. Popovitz-Biro, E. Lifshitz, and M. Lahav, *Adv. Funct. Mater.* **12**, 713 (2002).
- ²¹H. Cohen, S. K. Sarkar, and G. Hodes, *J. Phys. Chem. B* **110**, 25508 (2006).
- ²²H. Cohen, *J. Electron Spectrosc. Relat. Phenom.* **176**, 24 (2010).
- ²³O. Ö. Ekiz, K. Mizrak, and A. Dâna, *ACS Nano* **4**, 1851 (2010).
- ²⁴H. Sezen and S. Suzer, *J. Vac. Sci. Technol. A* **28**, 639 (2010).
- ²⁵H. Sezen, E. Ozbay, O. Aktas, and S. Suzer, *Appl. Phys. Lett.* **98**, 111901 (2011).
- ²⁶H. Sezen and S. Suzer, *J. Chem. Phys.* **135**, 141102 (2011).
- ²⁷Y. Wang and N. Herron, *J. Lumin.* **70**, 48 (1996).
- ²⁸H. Sezen and S. Suzer, *Surf. Sci.* **604**, L59 (2010).
- ²⁹F. W. Wise, *Acc. Chem. Res.* **33**, 773 (2000).
- ³⁰S. Zhang, P. W. Cyr, S. A. McDonald, G. Konstantatos, and E. H. Sargent, *Appl. Phys. Lett.* **87**, 233101 (2005).
- ³¹G. Konstantatos, L. Levina, A. Fischer, and E. H. Sargent, *Nano Lett.* **8**, 1446 (2008).
- ³²J. M. Luther, M. Law, Q. Song, C. L. Perkins, M. C. Beard, and A. J. Nozik, *ACS Nano* **2**, 271 (2008).